LA-UR-17-20353
Approved for public release; distribution is unlimited.

Title: Neutron & Gamma Correlations using CGM in MCNP 6.2.0

Author(s): Anderson, Casey Alan
Mckinney, Gregg Walter
Tutt, James Robert

Intended for: 2017 ANS Annual Meeting, 2017-06-10 (San Fransisco, California, United States)

Issued: 2017-01-19 (Draft)

Neutron & Gamma Correlations using CGM in MCNP 6.2.0

C. A. Anderson*, G. W. McKinney, J. R. Tutt

* *NEN-5, Systems Design and Analysis, Los Alamos National Laboratory, P.O. Box 1663, Los Alamos, NM, 87545*
casey_a@lanl.gov, gwm@lanl.gov, jtutt@lanl.gov

INTRODUCTION

The general-purpose Monte Carlo radiation-transport code MCNP6™ [1] came from the integration of MCNP5™ and MCNPX™ [2]. The most recent release of MCNP, version 6.2.0, is scheduled for release in early 2017, which includes a variety of bug fixes and new features to the code.

MCNP traditionally models nuclear reactions using Monte Carlo sampling techniques on measured and modeled cross-sectional data contained within ACE (A Compact Evaluated Nuclear Data File) libraries. In addition to reaction cross-sections, ACE libraries contain information relating to the production of secondary particles, such as secondary neutrons and photons. For example, an incident neutron on a nucleus can produce a nuclear reaction in the form $(n, M_n n')$, where n is the incident neutron and M_n is the number of secondary neutrons n' produced. Using this notation, different reactions can be described based on their neutron multiplicity, such as neutron capture ($M_n = 0$), elastic and inelastic scattering ($M_n = 1$), and reactions with multiple secondary neutrons ($M_n > 1$). In addition to secondary neutrons, these reactions can emit secondary γ-rays from the residual nuclei. Therefore, these reactions can be further generalized as $\left(n, M_n n' M_\gamma \gamma\right)$, describing a reaction producing M_n secondary neutrons and M_γ secondary γ-rays, referred to as the neutron and γ multiplcities, respectively. ACE libraries contain the cross-sectional data for each reaction, and their corresponding statistically averaged multiplicities for neutrons and photons, $\overline{M}_n$ and $\overline{M}_\gamma$.

However, there are several limitations to reaction sampling using ACE libraries. First, the data contained within ACE libraries is limited by the accuracy of the model and/or experiment, which out of necessity can greatly simplify the true physics behind a reaction. For example, in the $\left(n, M_n n' M_\gamma \gamma\right)$ reaction described above, the number of secondary γ-rays is described by the statistically averaged multiplicity $\overline{M}_\gamma$ instead of a distribution. Consequently, MCNP is unable to produce a continuous distribution, and instead utilizes a binary sampling distribution around $\overline{M}_\gamma$. While this sampling method provides an accurate representation of the statistically average M_γ over a large simulation, it is an inaccurate representation of an individual reaction and its corresponding secondary particles. Secondary neutrons are affected in a similar manner, such that different kinds of secondary neutrons can be sampled from the same interaction (eg., an inelastic neutron with an $[n, 2n]$ neutron). Lastly, the random sampling technique for secondary particles remains completely independent of the sampled reaction, eliminating the ability to correlate secondary particles for a given reaction.

To supplement these data libraries, additional codes and models describing certain nuclear reactions are employed. These codes can fill in the information missing from ACE, provide a better model to the true physics distribution, and can provide true correlated secondary particles, which has many useful applications in research and industry [3, 4, 5, 6].

Cascading Gamma-ray and Multiplicity (CGM) code

One such example of a code implemented in MCNP is the CGM code. Originally developed in MCNPX V2.7.0 [7] and integrated in MCNP6, the CGM code was developed to study β-delayed neutrons, prompt fission neutrons, and γ-ray emissions based on the Hauser-Feshbach statistical model [8]. With this original implementation, CGM provided both a broader distribution of γ-multiplicities for each reaction and allowed correlation of secondary γ-rays through its combination of Monte Carlo and determinstic methods.

However, the initial MCNP implementation of CGM only modeled the secondary γ-rays, while secondary neutrons were still handled using ACE libraries. As such, secondary neutrons were limited by the same problems facing secondary γ-rays using ACE interactions, including an inability to correlate these secondary neutrons for each reaction. With the release of MCNP 6.2.0, the CGM code has been modified to return secondary neutrons, providing an ability to correlate secondary neutrons and γ-rays following a reaction.

For a detailed background of CGM and its previous implementation in MCNP, please refer to Kawano et al. [9] and Wilcox et. al [7, 10]. A brief summary of CGM, along with its new modifications released in MCNP 6.2.0, is summarized here.

METHODS

CGM in MCNP 6.2.0

The CGM code is activated in MCNP by setting the 9th entry on the neutron `PHYSICS` data card, which controls secondary particle production for neutron reactions, to "2":

```
PHYS:N   8j   2
```

Additional options for this value include "1", which retains the default option using ACE library sampling, or "0" to turn off secondary particle production. Note that this entry differs from the implementation in MCNPX V2.7.0, where the 8th entry controlled the use of CGM.

When CGM is activated, elastic scattering and reactions with materials of $Z < 9$ continue using ACE libraries for secondary particle production. For non-elastic interactions with nuclides of $Z > 9$, the production of secondary particles is modeled using CGM.

New to MCNP 6.2.0 when the CGM option is specified, all neutron capture events are forced into analog capture. This

ensures that the primary particle is killed, and all neutrons transported after the reaction are directly created using CGM. For the simulated reaction, the calculation of the excitation energy E_x is given by:

$$E_x = \frac{A_{In}}{A_{In} + m_{In}} Elab_{In} + BE \quad (1)$$

where A_{In}, m_{In}, and $Elab_{In}$ are the target nucleus mass, incident particle mass, and particle energy in the lab frame, respectively, and BE represents the binding energy of the incident neutron. In the previous version of CGM, the excitation energy E_x was reduced by an additional term $\left(\sum_{i=1}^{2} \frac{A_i}{A_i+m_i} Elab_i\right)$ to account for the secondary neutrons that were not modeled using CGM. Now that secondary neutrons are determined using CGM, this term is omitted and the full excitation energy is passed to CGM. Another modification from the original CGM implementation is the substitution of the reaction Q-value with the neutron binding energy for calculating the excitation energy passed to CGM. For this preliminary application, the neutron binding energy was set at 8.5 MeV (an average value for stable nuclides 9<Z<90).

The excitation energy E_x and the Z/A of the excited nucleus are passed to the CGM code, which uses emission probabilities and methods described in Wilcox et. al ([7]) to calculate secondary neutrons and γ-rays and their respective energies. These particles are passed back to MCNP from CGM and sampled isotropically in the center-of-mass frame.

Examples

Several examples of the neutron and γ-multiplicity correlations were tested in this report; 10 MeV neutrons on a low-Z material (^{28}Si), 20 MeV neutrons on a mid-Z material (^{56}Fe), 1 eV and 16 MeV neutrons on a high-Z material (^{207}Pb). For each case, two separate runs were performed, one using ACE sampling and one using CGM. To correlate the distribution of secondary neutrons and γ-rays, only first interactions were simulated by setting the 8th entry on the LCA card to -2, and a pulse-height light (PHL) tally was utilized for coincident counting of neutrons and photons. An example of the MCNP input deck for the 16 MeV neutrons on ^{207}Pb is provided in the Appendix.

RESULTS

The energy spectra for secondary neutrons and photons are shown in Figure 1. Elastic scattering peaks are located at the upper end of the energy spectra near the incident energy, and should have very similar distributions at this energy as it is only handled by ACE libraries, even when CGM is activated. The secondary neutron spectra from 20 MeV neutrons on ^{56}Fe are compared with the results from the CoH code by Kawano et, al [9], a superset of the CGM code.

The correlated neutron and γ multiplicities M_n and M_γ are provided in Figure 2, showing the unique distributions for ACE (left column) and CGM (right column) for the selected examples. For all examples, CGM provides more discrete values of M_γ, including up to twelve discrete secondary γ-rays. In contrast, ACE libraries are limited to a binary integer

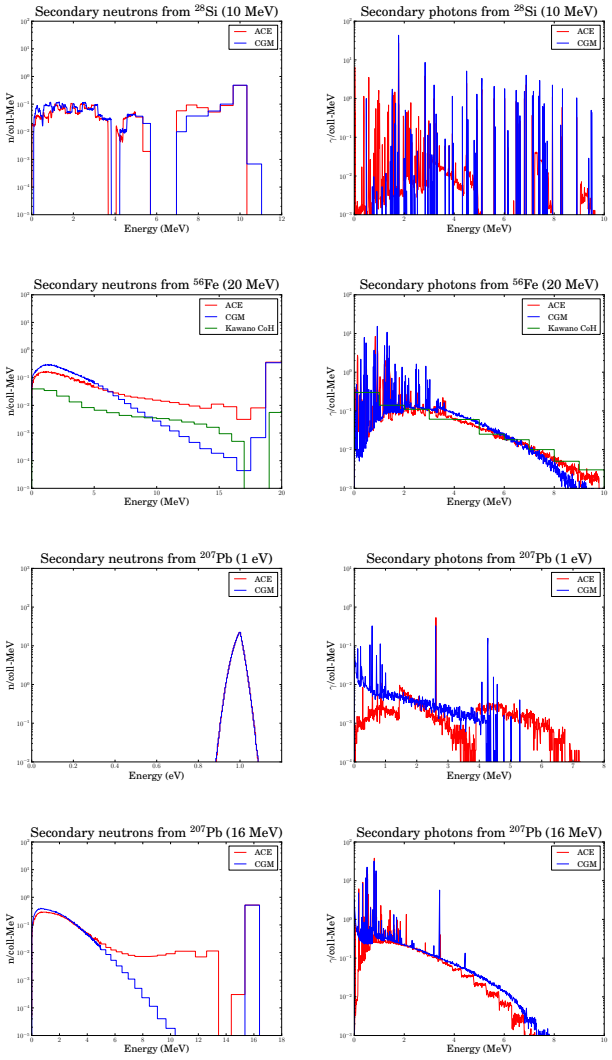

Fig. 1: Secondary neutron (left column) and gamma (right column) spectra for CGM (blue) and ACE (red) for energetic neutrons on different materials. The CoH results are shown in green for the 20 MeV neutrons on ^{56}Fe.

distribution of M_γ above and below $\overline{M}_\gamma$. The high-Z materials provide more discrete secondary γ-rays compared to low-Z and mid-Z materials, even for slow 1 eV neutrons. Note that a neutron multiplicity of one $\left(n, n' M_\gamma \gamma\right)$ corresponds to elastic scatter ($M_\gamma = 0$), inelastic scatter ($M_\gamma > 0$), and neutron capture with a single neutron emission (e.g $[n, n' p]$). Elastic scattering is one of the dominate reactions for low-Z materials and for the slow 1 eV neutrons.

CGM provides unique M_γ distributions for each M_n, whereas ACE sampling provides the same normalized distribution and $\overline{M}_\gamma$ for all M_n. The average $\overline{M}_\gamma$ for each M_n is summarized in Table I for the 16 MeV neutrons on ^{207}Pb example (bottom row, Figure 2). In this example, CGM shows a high $\overline{M}_\gamma$ for $M_n = 0$ and $M_n = 2$, with near zero for $M_n = 1$ and $M_n = 3$. The near zero $\overline{M}_\gamma$ for $M_n = 1$ demonstrates that elastic scattering ($M_\gamma = 0$) dominates relative to inelastic

		M_n			
		0	1	2	3
$\overline{M}_\gamma$	ACE	2.00	2.00	2.00	2.00
	CGM	5.49	0.04	5.56	0.62

TABLE I: Average γ-multiplicities $\overline{M}_\gamma$ for different neutron-multiplicities M_n for fast neutrons on ^{207}Pb.

scattering ($M_\gamma > 0$), which can be inferred using CGM and not with ACE.

Mat.	Energy (MeV)	*rxn*	$\overline{M}_n$	$\overline{M}_\gamma$
^{28}Si	10	ACE	0.75	0.88
		CGM	0.75	1.03
^{56}Fe	20	ACE	1.22	1.18
		CGM	1.47	1.33
^{207}Pb	1e-6	ACE	0.99	0.02
		CGM	0.99	0.04
^{207}Pb	16	ACE	1.40	2.00
		CGM	1.48	2.35

TABLE II: Average neutron ($\overline{M}_n$) and γ ($\overline{M}_\gamma$) multiplicities for selected materials and incident neutron energies.

A summary of all the average neutron and γ multiplicities $\overline{M}_n$ and $\overline{M}_\gamma$ for all the examples is provided in Table II, obtained by integrating over all M_n and M_γ. Comparable values are seen for both ACE and CGM.

Using CGM, the computational performance, measured by the figure-of-merit value provided in MCNP, was decreased by one to two orders of magnitude compared to ACE sampling.

CONCLUSIONS

The CGM code has been modified in MCNP 6.2.0 to return both secondary neutrons and photons, allowing correlation of these secondary particles following a given reaction.

ACKNOWLEDGMENTS

This work has been supported by the U.S. Department of Homeland Security, Domestic Nuclear Detection Office, under competitively awarded contract/IAA HSHQDC-12-X-00251. This support does not constitute an express or implied endorsement on the part of the Government.

APPENDIX

```
1 1 -11.34   -1  imp:n=1
2 0           1  imp:n=0

1 so 1.0

mode n p
m1  82207 1
phys:n 20 7j 2
cut:n,p 2j 0 0
lca 7j -2
sdef par=n erg=16.078 $ 16 MeV in COM
f1:n 1
e1  .005 498i 4.995 20log 20
f31:p 1
e31 .001 998i 10
f11:n 1
f21:p 1
f8:n,p 1
ft8 PHL 1 11 1  1 21 1  0
e8  0.5 1.5 2.5 3.5
fu8 0.5 1.5 2.5 3.5 4.5 5.5 6.5 7.5
    8.5 9.5 10.5 11.5 12.5
fq8 u e
print
nps 100000
```

REFERENCES

1. D. PELOWITZ, A. FALLGREN, and G. MCMATH, "MCNP6 User's Manual, Version 6.1.1beta," *LANL report LA-CP-14-00745* (2014).
2. D. PELOWITZ, "MCNPX User's Manual, Version 2.7.0," *LANL report LA-CP-11-00438* (2014).
3. J. DRAPER and T. SPRINGER, "Multiplicity of Resonance Neutron Capture Gamma Rays," *Nuclear Physics*, **16**, 27–37 (1960).
4. R. LINDSTROM, "Prompt-gamma activation analysis and application in industry, environment, and medicine," *Acta Physica Hungarica*, **75**, 71–76 (1994).
5. R. ODOM, S. BAILEY, and R. WILSON, "Benchmarking Computer Simulations of Neutron-induced, Gamma-ray Spectroscopy for Well Logging," *Applied Radiation and Isotopes*, **48**, 1321–1328 (1997).
6. C. DEYGLUN and ET. AL, "Passive and Active Correlation Techniques for the Detection of Nuclear Materials," *IEEE Transactions on Nuclear Science*, **61**, 2228–2234 (2014).
7. T. WILCOX, T. KAWANO, G. MCKINNEY, and J. HENDRICKS, "Correlated gammas using CGM and MCNPX," *Progress in Nuclear Energy*, **63**, 1–6 (2013).
8. W. HAUSER and H. FESHBACH, "The inelastic scattering of neutrons," *Physical Review*, **87**, 366–373 (1952).
9. T. KAWANO, P. TALOU, M. CHADWICK, and T. WATANABE, "Monte Carlo Simulation for Particle and Gamma-Ray Emissions in Statistical Hauser-Feshbach Model," *Journal of Nuclear Science and Technology*, **47**, *5*, 462–469 (2010).
10. T. WILCOX, G. MCKINNEY, and T. KAWANO, "MCNP6 Gets Correlated with CGM 3.4," *ANS RPSD 2014 - 18th Topical Meeting of the Radiation Protection and Shielding Division of ANS*, pp. 1–3 (2014).

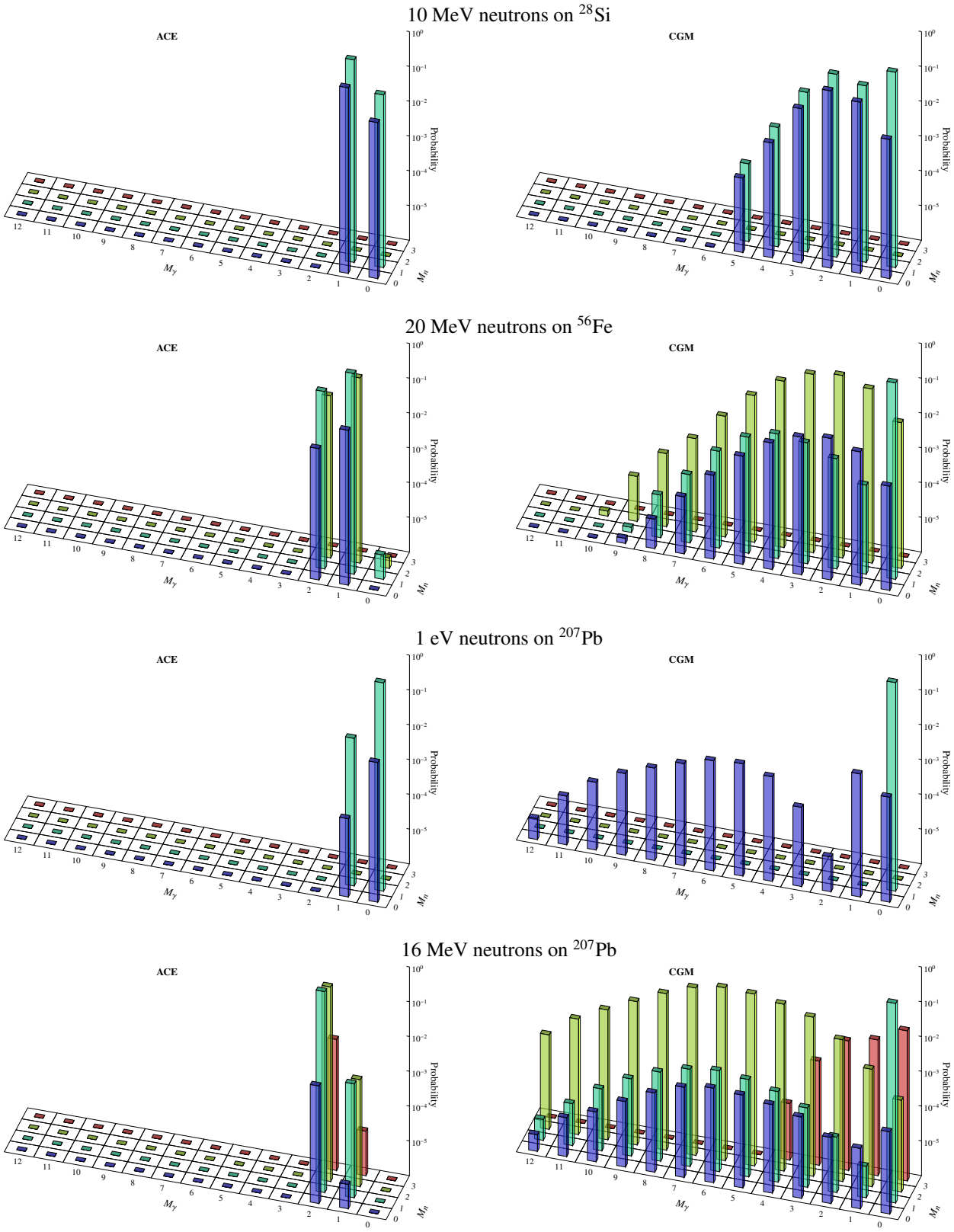

Fig. 2: Correlated multiplicity distributions for ACE (left column) and CGM (right column) for selected cases.